

Thermal segregation of intruders in the Fourier state of a granular gas

J. Javier Brey and Nagi Khalil

*Física Teórica, Universidad de Sevilla,
Apartado de Correos 1065, E-41080 Sevilla, Spain*

James W. Dufty

Department of Physics, University of Florida, Gainesville, FL 32611, USA

(Dated: November 4, 2018)

Abstract

A low density binary mixture of granular gases is considered within the Boltzmann kinetic theory. One component, the intruders, is taken to be dilute with respect to the other, and thermal segregation of the two species is described for a special exact solution to the Boltzmann equation. This solution has a macroscopic hydrodynamic representation with a constant temperature gradient and is referred to as the Fourier state. The thermal diffusion factor characterizing conditions for segregation is calculated without the usual restriction to Navier-Stokes hydrodynamics. Molecular dynamics simulations are reported for comparison with the results for this idealized Fourier state.

PACS numbers: 45.70.Mg, 05.20.Dd

I. INTRODUCTION

Segregation among species in a granular mixture is of significant practical importance, and its description, both qualitative and quantitative, a challenging problem [1]. Many physical systems and state conditions are of interest, involving a range of mechanisms responsible for segregation across a wide range of control parameters. Here, attention is focused on a simple system of gas mixtures in a temperature gradient, being the latter the only mechanism available to induce segregation. Furthermore, each species is assumed to be composed of smooth, inelastic hard spheres at low density, so the inelastic Boltzmann kinetic equation applies [2]. One component (the impurities) is taken to be dilute with respect to the other (the host). In this limit the host gas is not affected by the impurities, and is described by its own independent Boltzmann equation.

The macroscopic balance equations, or hydrodynamic equations, obtained from this kinetic theory description have special exact solutions: the host gas has zero flow velocity, a constant temperature gradient and a constant pressure [3, 4]; the impurity gas has zero flow velocity, a temperature proportional to the host temperature, and a pressure proportional to a power of that temperature [5]. Since the heat flux of the host component can be expressed as proportional to the temperature gradient, i.e. by Fourier's law, this state is referred to here as the Fourier state. The coefficients in this hydrodynamic description are defined in terms of coupled, nonlinear integral equations obtained from kinetic theory. In this way, an exact description of a mixture in a temperature gradient is obtained as the basis for exploration of segregation as a function of the temperature gradient and differences in mechanical properties of the two species. No explicit limitations on the magnitude of the temperature gradient are assumed in this analysis and all higher degree derivatives are exactly zero. This complements the extensive studies of thermal segregation based on applications of kinetic theory at the Navier-Stokes level [6, 7].

Due to the symmetry of the problem, all spatial variation of properties occurs along the temperature gradient, taken to be the x axis. The segregation of impurity particles relative to the host gas is described by the variation of the composition $n_0(x)/n(x)$, where $n_0(x)$ and $n(x)$ are the impurity and host densities, respectively. In the absence of the temperature gradient, these densities are uniform and there is no segregation. For a finite temperature gradient, a convenient measure of thermal segregation is given in terms of the

thermal diffusion factor Λ defined by

$$\frac{d}{dx} \ln \frac{n_0(x)}{n(x)} = -\Lambda \frac{d \ln T(x)}{dx}. \quad (1)$$

For the special hydrodynamic state constructed here this dimensionless factor is independent of x and therefore a global property of the system. For more general states, Λ is a local function and segregation properties can vary throughout the system. Here, it can depend only on a dimensionless form of the temperature gradient as well as ratios of the mechanical properties of each species (size, mass, degree of collisional inelasticity). It can be positive or negative, implying that the impurity concentration increases against or along the temperature gradient, respectively (a thermal analogue of the Brazil nut and reverse Brazil nut effects for gravitational segregation [8–11]). Of course, Λ should vanish for mechanically identical host and impurity particles.

The expression for Λ depends on coefficients defining the hydrodynamic fields which in turn are defined in terms of solutions to nonlinear integral equations following from the underlying kinetic theory. The kinetic theory and associated hydrodynamics for the Fourier state has been described elsewhere [5], so only a brief summary is presented in the next section. An analytic solution to the integral equations can be obtained as described in [5], and the results are extended here to arbitrary dimension d in the Appendix. More generally, for arbitrary degree of inelasticity the equations are solved by a truncated Sonine polynomial expansion [4, 5]. The results in both cases for Λ and the violation of energy equipartition measured by means of the parameter $\gamma \equiv T_0/T$, are illustrated for a wide range of degrees of inelasticity (granular and non-equilibrium systems violate the equipartition property of equilibrium states and hence the steady temperatures of the two systems are different in general). Next, event driven molecular dynamics simulations (MD) are described for 200 inelastic hard disks ($d = 2$) in a rectangular box with thermal walls to generate a temperature gradient. The Fourier state spatial dependence of the hydrodynamic fields for both species is confirmed in the bulk of the system, away from boundary layers near the walls. Comparison of the MD and Fourier state results for the temperature ratio γ as a function of dissipation, mass ratio, and size ratio shows good agreement only for weak to moderate dissipation, or small mechanical differences, but only qualitative agreement is found otherwise. This poor accuracy is interpreted as a limitation of the Sonine approximation for this property. However, MD and Fourier state results for the thermal diffusion factor Λ show much better

agreement over the entire parameter space. These results are discussed further in the last section.

II. THE FOURIER STATE FOR THE HOST GAS AND THE IMPURITIES

Consider a system of N smooth inelastic hard spheres ($d = 3$) or disks ($d = 2$) of mass m and diameter σ . Inelasticity of collisions is characterized by a constant, velocity independent, coefficient of normal restitution α , defined in the interval $0 < \alpha \leq 1$. Then, when two particles, i and j , with velocities \mathbf{v}_i and \mathbf{v}_j collide, the velocities are instantaneously modified to new values given by

$$\begin{aligned} \mathbf{v}'_1 &= \mathbf{v}_1 - \frac{1 + \alpha}{2}(\mathbf{g} \cdot \hat{\boldsymbol{\sigma}})\hat{\boldsymbol{\sigma}}, \\ \mathbf{v}'_2 &= \mathbf{v}_2 + \frac{1 + \alpha}{2}(\mathbf{g} \cdot \hat{\boldsymbol{\sigma}})\hat{\boldsymbol{\sigma}}, \end{aligned} \quad (2)$$

where $\mathbf{g} \equiv \mathbf{v}_1 - \mathbf{v}_2$ and $\hat{\boldsymbol{\sigma}}$ is the unit vector joining the centers of the two particles at contact. The system is supposed to be very dilute, so that the one-particle distribution function for position \mathbf{r} and velocity \mathbf{v} at time t , $f(\mathbf{r}, \mathbf{v}, t)$, obeys the inelastic Boltzmann equation [2]. In [3, 4] a special solution of this equation was proposed, and the state associated with it was called the Fourier state. It is a time-independent distribution function with gradients only in one direction and having a scaling form in terms of the hydrodynamic fields,

$$f(x, \mathbf{v}) = n(x) \left[\frac{m}{2T(x)} \right]^{d/2} \phi(\mathbf{c}), \quad \mathbf{c} \equiv \left[\frac{m}{2T(x)} \right]^{1/2} \mathbf{v}. \quad (3)$$

In the above expressions, T is the granular temperature and n is the number of particles density. Both are defined from the one-particle distribution function in the usual way, although with the Boltzmann constant set equal to unity. It is verified that the state defined by the above distribution has a uniform hydrodynamic pressure $p \equiv n(x)T(x)$, a heat flux q_x proportional to $T(x)^{1/2}$, and it exhibits a linear temperature profile,

$$\frac{dT(x)}{dx} = Bp\sigma^{d-1}, \quad (4)$$

with the dimensionless constant B given by a functional of ϕ [3, 4]. This functional, as well as the function ϕ , was approximately determined by solving the Boltzmann equation using a representation of the distribution function ϕ as a truncated Sonine polynomial expansion, and keeping only up to bilinear terms in the coefficients [4]. The results were shown to be

in good agreement with molecular dynamics simulation data, at least for weak inelasticity ($0.9 \leq \alpha < 1$).

Now suppose that M additional hard spheres or disks of mass m_0 and diameter σ_0 are added to the host gas in the Fourier state. For $M \ll N$, the effect of these “impurity” particles or “intruders” on the host gas distribution function is negligible, so that the results described above remain valid. Moreover, the dynamics of the impurities is determined by their collisions with the host gas particles, while collisions between intruders can be neglected. When an intruder with velocity \mathbf{v}_0 collides with a gas particle of velocity \mathbf{v}_1 , the velocities are instantaneously changed into

$$\begin{aligned}\mathbf{v}'_0 &= \mathbf{v}_0 - \frac{m(1 + \alpha_0)}{m + m_0} (\mathbf{g}_0 \cdot \hat{\boldsymbol{\sigma}}) \hat{\boldsymbol{\sigma}}, \\ \mathbf{v}'_1 &= \mathbf{v}_1 + \frac{m_0(1 + \alpha_0)}{m + m_0} (\mathbf{g}_0 \cdot \hat{\boldsymbol{\sigma}}) \hat{\boldsymbol{\sigma}},\end{aligned}\tag{5}$$

where $\mathbf{g}_0 \equiv \mathbf{v}_0 - \mathbf{v}_1$ and α_0 is the coefficient of normal restitution for collisions between an intruder and a host gas particle. It is also defined in the interval $0 < \alpha_0 \leq 1$. In the tracer limit being considered, the one-particle distribution function for the additional particles, $F(\mathbf{r}, \mathbf{v}_0, t)$, obeys the inelastic Boltzmann-Lorentz equation [5, 12]. A solution of this equation similar to (3) is considered,

$$F(x, \mathbf{v}_0) = n_0(x) \left[\frac{m_0}{2\gamma T(x)} \right]^{d/2} \Phi(\mathbf{c}_0), \quad \mathbf{c}_0 \equiv \left[\frac{m_0}{2\gamma T(x)} \right]^{1/2} \mathbf{v}_0.\tag{6}$$

Here n_0 is the number density of intruders and the function Φ has been chosen such that the average velocity vanishes and the granular temperature of the impurities, defined from the second velocity moment of F , is $T_0(x) = \gamma T(x)$. The parameter γ , measuring the deviation from energy equipartition, must be identified (similarly to the function Φ) by requiring Eq. (6) to be a solution of the Boltzmann-Lorentz kinetic equation. A necessary condition for it is that [5]

$$\frac{d \ln n_0(x)}{dx} = C n(x) \bar{\sigma}^{d-1},\tag{7}$$

with $\bar{\sigma} \equiv (\sigma + \sigma_0)/2$ and C being a constant. The distribution function Φ and the constant C have also been evaluated by using a truncated Sonine representation for ϕ and Φ [5]. The distribution function F is “normal” in the context of kinetic theory, i.e. it depends on position only through the local densities and the temperature of the system.

As already mentioned in the Introduction, the main focus in this paper is on segregation, i.e. the demixing of the granular mixture, by thermal diffusion. The amount of segregation

can be measured by the thermal diffusion factor Λ defined by (1). The value $\Lambda = 0$ indicates that no segregation induced by the temperature gradient occurs, in the sense that the density ratio does not depend on position. On the other hand, when $\Lambda > 0$ the impurity concentration increases against the temperature gradient, while for $\Lambda < 0$ the impurity concentration increases as the temperature increases. By means of Eqs. (4) and (6) the thermal diffusion factor can be expressed in the present case as

$$\Lambda = - \left(1 + \frac{\bar{\sigma}^{d-1} C}{\sigma^{d-1} B} \right). \quad (8)$$

For arbitrary values of the restitution coefficients, the equations determining the coefficients of the truncated Sonine expansions of the distribution functions are rather involved (even in the bilinear approximation used in refs. [4] and [5]) and they must be solved numerically. Nevertheless, in the limit of small inelasticity for the host gas, i.e. $1 - \alpha \ll 1$, it is possible to obtain explicit expressions for the coefficients. The results are summarized in the Appendix. In Figs. 1 and 2, the asymptotic expressions for Λ and γ for small inelasticity of the host gas, as given in the Appendix, are compared with the numerical solution of the kinetic equations. The comparison is carried out as a function of the coefficient of inelasticity α for several values of α_0 , as indicated in the figures. The constant values of the other parameters are $d = 2$, $m_0 = m$, and $\sigma_0 = \sigma$. It is important to realize that all the expressions being compared have been obtained in the Sonine approximation and neglecting products of three or more of the coefficients appearing in the truncated expansion of the distribution function. Consequently, nothing can be concluded about the validity of the truncated Sonine approximation from those figures. It is seen that the accuracy of the asymptotic expression for the temperature ratio extends up to smaller values of the coefficient α than the corresponding expression for the thermal diffusion factor. Actually, the latter does not depend on α in the considered limit. This behavior was to be expected since, as pointed out in the Appendix, the former has been evaluated to order $1 - \alpha$ and the latter to order $(1 - \alpha)^{1/2}$. Similar results are obtained for inelastic hard spheres ($d = 3$).

III. MOLECULAR DYNAMICS SIMULATIONS

Event driven molecular dynamics simulations of a system of inelastic hard disks ($d = 2$) have been performed to check the accuracy of the above theoretical predictions. In all the

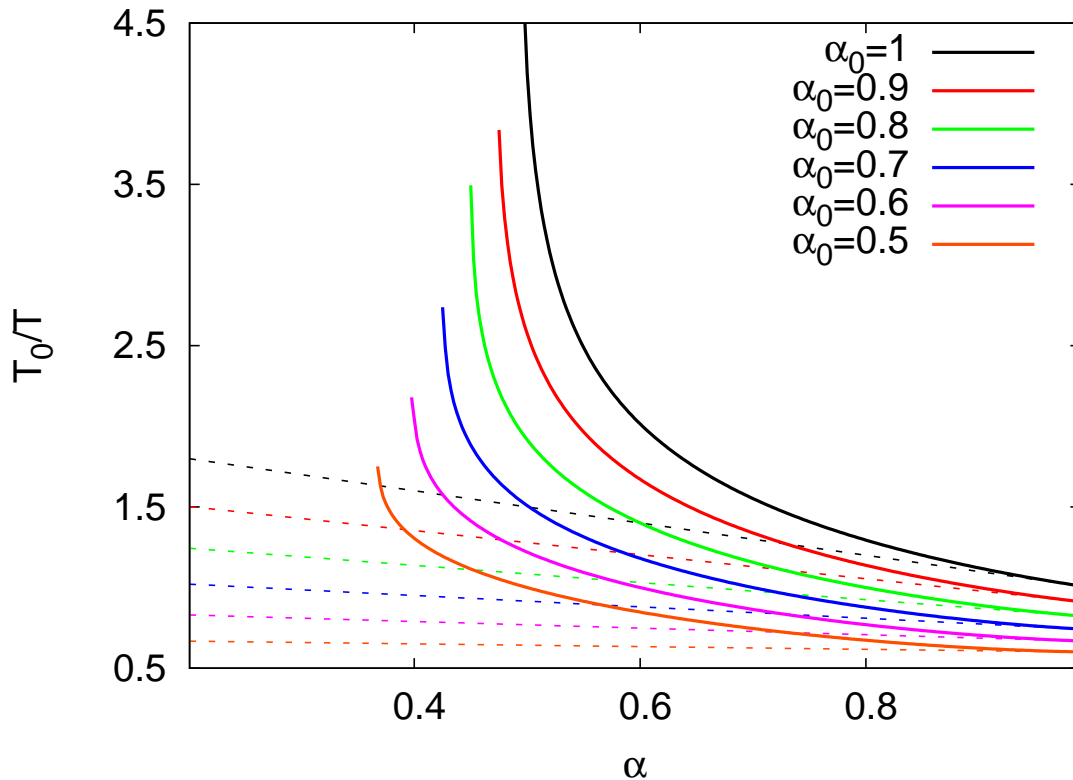


FIG. 1: (Color on line) Temperature of the impurities T_0 divided by the temperature of the host gas T as a function of the coefficient of normal restitution of the gas particles α , for several values of the restitution coefficient for collisions between the gas particles and the impurities, α_0 , as indicated in the insert (the lower the curve the smaller α_0). In all cases, $d = 2$, $m_0 = m$, and $\sigma = \sigma_0 = \bar{\sigma}$. The solid lines have been obtained by solving numerically the Boltzmann equation in the Sonine approximation, while the dashed ones are the expressions in the almost elastic host gas limit given in the Appendix.

simulations to be reported, the number of particles is $N = 200$ and they are enclosed in a rectangular cell of sides $L_x = 4L_y = 200\sigma$. Moreover, only a single impurity was considered, i.e. $M = 1$. The simulations started with all the particles, including the impurity, uniformly distributed on a square lattice and with a Gaussian velocity distribution.

A. The Fourier state

To generate the Fourier state, the same procedure as in ref. [4] was employed. To inject energy into the system and induce the temperature gradient, two thermal walls [13, 14]

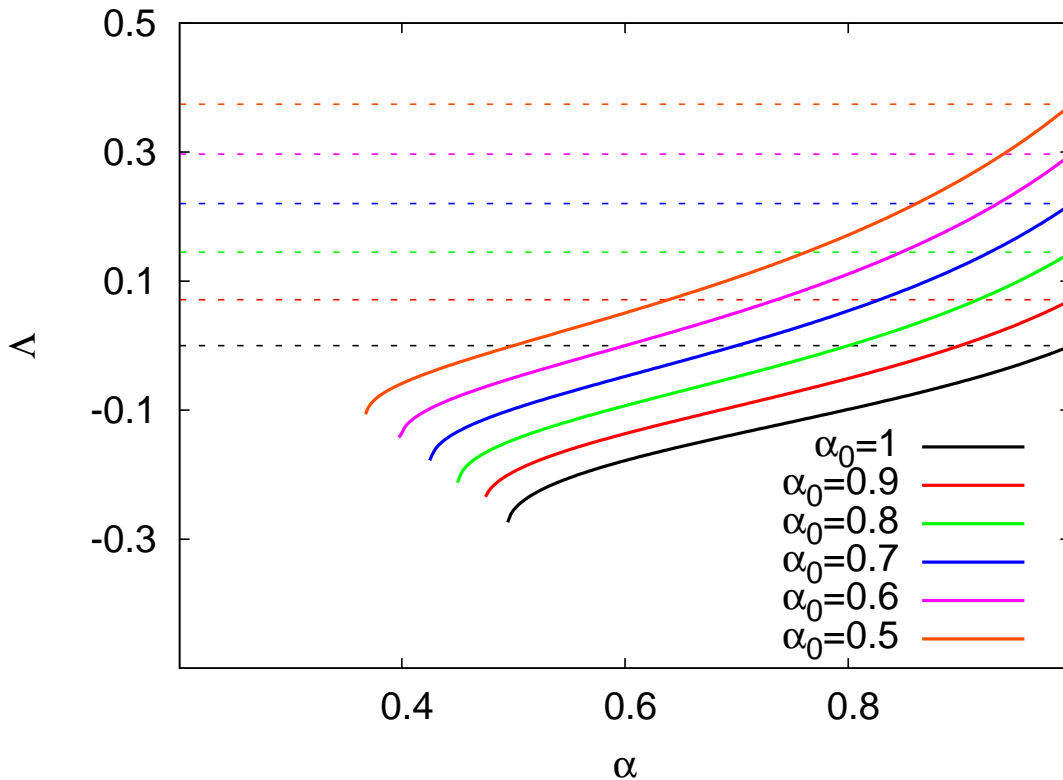


FIG. 2: (Color on line) The dimensionless thermal diffusion factor Λ as a function of the coefficient of normal restitution of the gas particles α , for several values of the restitution coefficient for collisions between the gas particles and the impurities, α_0 , as indicated in the insert (the lower the curve the larger α_0). In all cases, $d = 2$, $m_0 = m$, and $\sigma = \sigma_0 = \bar{\sigma}$. The solid lines have been obtained by solving numerically the Boltzmann equation in the Sonine approximation, while the dashed ones are the expressions in the almost elastic host gas limit given in the Appendix.

located at $x = 0$ and $x = L_x$ were considered, while periodic boundary conditions were used in the y direction. The temperatures of the walls were chosen accordingly with the theoretical prediction for the Fourier state [4]. For the cases being reported, it was found that the system reached, after a transient period, a steady state with gradients only in the x -direction and no macroscopic flow. This is consistent with the value chosen for the aspect ratio L_x/L_y , which is outside the region in which the transversal hydrodynamic instability exhibited by the state we are considering shows up [15, 16] for the parameters used in the simulations.

Figure 3 shows the pressure, temperature, and heat flux profiles measured in a system with $\alpha = 0.9$. The finite system generated by MD has boundary layers near $x = 0$ and

$x = L_x$, where a hydrodynamic description does not hold. Outside those layers a bulk region in which the pressure and the scaled heat flux are uniform while the temperature is linear is clearly identified. This is the region in which the theoretical predictions are expected to hold. For $\alpha > 0.9$ a similar behavior is observed, with the size of the bulk region increasing as α increases.

Once the system has reached the Fourier state, several properties of the gas and the impurity have been measured. The system has been divided in 20 slices parallel to the y axis of the same width. Moreover, the results that will be shown have been averaged in time, and also over 500 trajectories of the system. The emphasis has been put on the temperature and density profiles of both the gas and the impurity, and on the values of the parameters γ and Λ obtained from them. In order to get a systematic information of the role played by the several properties of the impurity $(\alpha_0, m_0, \sigma_0)$, only one of these properties is chosen in each case to differ from the gas host particles. Then, for instance, in those cases in which $\alpha \neq \alpha_0$, the values $m_0 = m$ and $\sigma_0 = \sigma$ have been employed.

The quantity $\gamma \equiv T_0/T$ has been computed by identifying the bulk region of the system in which the temperature ratio is homogeneous. An example for $\alpha = 0.99$ is given in Fig. 4. The different data sets correspond to vary one of the parameters of the impurity as indicated in the insert. In each of the cases, all the others parameters are the same for the host gas particles and for the impurity. It is seen that the ratio is uniform over most of the system. The deviation from unity is small for the differences in mass and size ratios considered since the system is almost elastic in all collisions. However, when there is a large difference between the two coefficients of normal restitution a rather strong violation of energy equipartition shows up. This is a general property of granular mixtures [8, 17–19]. The values of γ reported in the following have been obtained by averaging the temperature ratio in the region in which it is roughly uniform.

The coefficient Λ could be measured, in principle, by using its definition in Eq. (1). Nevertheless, the measurement of temperatures from the simulation data introduces more uncertainties than the measurement of densities. Taking into account that in the Fourier state the pressure is uniform, Eq. (1) can be transformed into

$$\Lambda = \frac{d \ln n_0}{d \ln n} - 1. \quad (9)$$

This is the expression actually used to compute Λ , i.e. it is obtained from the slope of linear

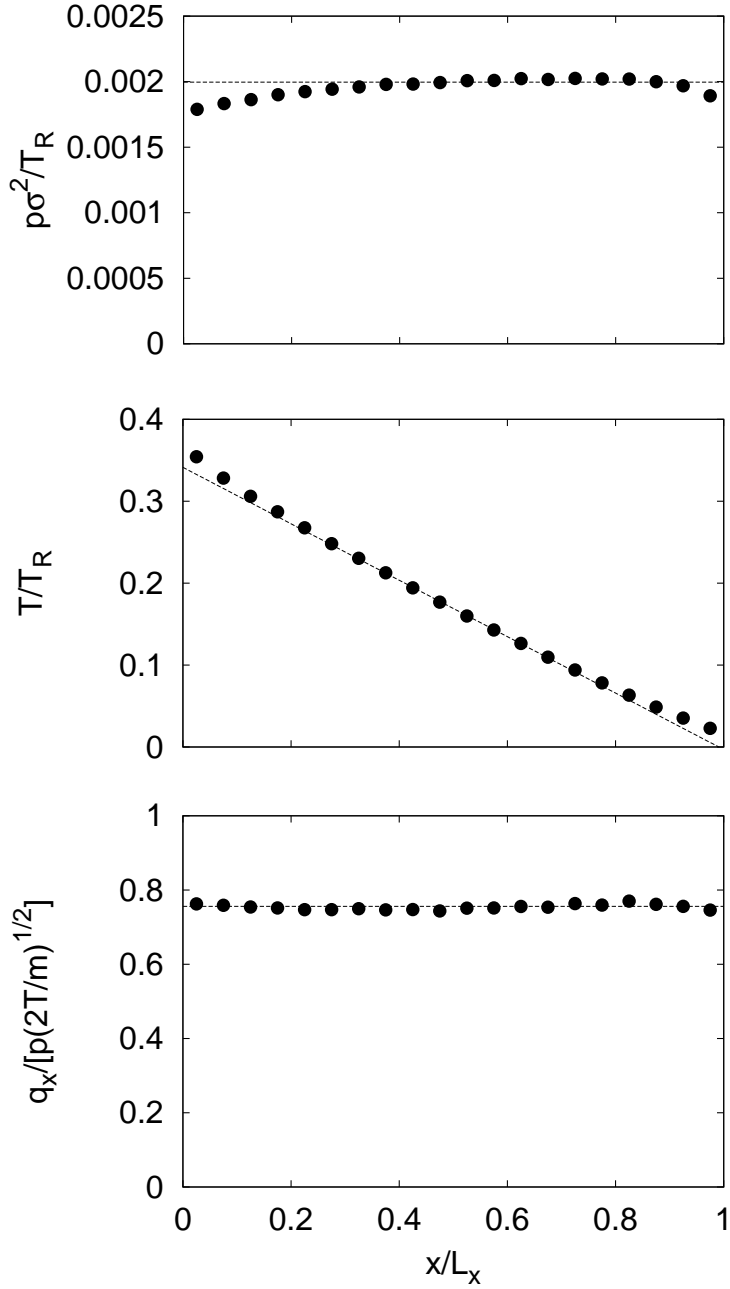


FIG. 3: Steady dimensionless pressure, temperature and heat flux profiles for a system of hard disks with $\alpha = 0.9$. The mechanical properties of the impurity are the same as those of the host gas particles. The temperature and pressure have been scaled with some arbitrary reference value, T_R , actually the initial temperature of the system. The symbols are simulation data, the dashed straight lines in the pressure and heat profiles are guides for the eye, and the dashed line in the temperature profile is a linear fit of the data in the bulk of the system.

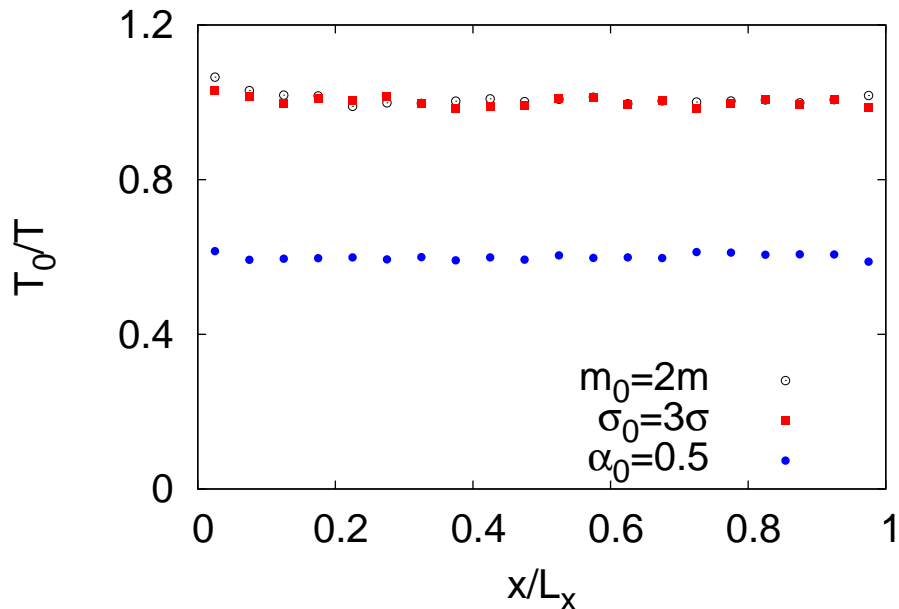


FIG. 4: (Color on line) Profile along the x direction of the ratio between the temperature of the intruder T_0 and the temperature of the system T for a system with $\alpha = 0.99$.

profile of $\ln n_0$ as a function of $\ln n$. An example is provided in Fig. 5. The three sets of data correspond to the intruder differing from the host gas particles in the mechanical property indicated in the insert.

B. Comparisons for γ and Λ

In the following, results will be restricted to the case $\alpha = 0.9$. Figures 6 and 7 show the behavior of γ as a function of α_0 ($m = m_0$ and $\sigma = \sigma_0$) and of m_0/m ($\alpha = \alpha_0$ and $\sigma = \sigma_0$), respectively. A good agreement between the theoretical predications and the simulation data is observed, although quantitative discrepancies in γ appear for small values of α_0 , i.e. very inelastic intruder. Figure 7 demonstrates the existence of segregation. The thermal diffusion coefficient is positive when $\alpha_0 < 0.9$, i.e. the impurity concentration is higher at the colder part of the system. For larger values of α_0 , segregation occurs in the opposite direction; the impurity concentration is higher in the hotter part of the system. Consistently, the value of α_0 for which the direction of the segregation effect changes is also the value at which the temperature of the impurity equals the temperature of the host gas, since at this point the intruder is equivalent to the gas particles.

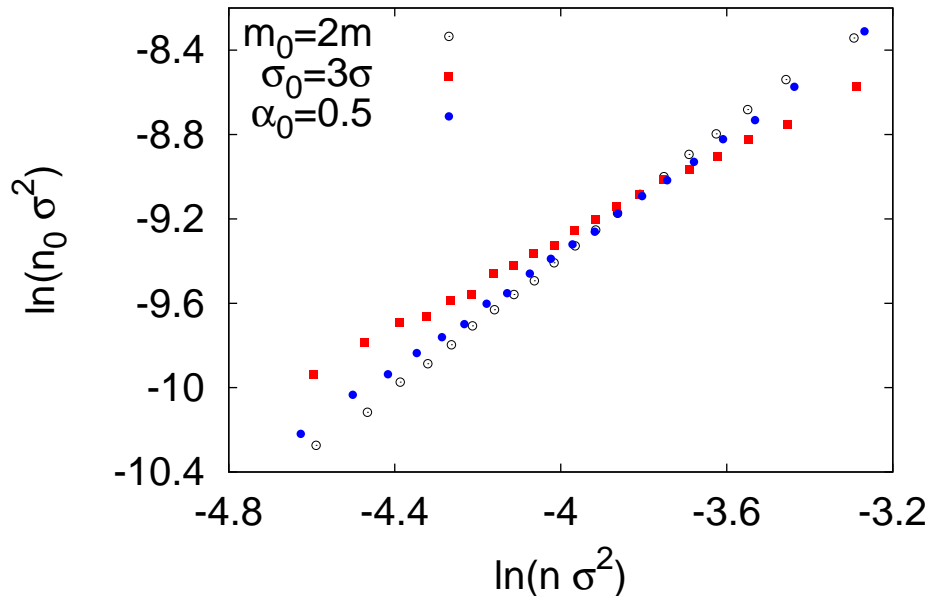


FIG. 5: (Color on line) Logarithm of the (dimensionless) intruder density as a function of the logarithm of the host gas (dimensionless) density, for a system with $\alpha = 0.99$.

The dependence on the mass ratio of both γ and Λ is shown in Figs. 8 and 9, respectively. Now it is observed that while the theory accurately predicts the thermal diffusion factor, it clearly fails to describe the breakdown of the energy equipartition. When the mass m_0 of the intruder is larger than the mass m of the host gas particles, the simulation results indicate that T_0/T grows rather fast with m_0/m , while the theory predicts a weak decrease remaining smaller than unity. Violations of energy equipartition in homogeneous granular mixtures much stronger than predicted by the existing kinetic theory models have been reported lately [19].

Finally, the dependence of γ and Λ on the diameter ratio σ_0/σ is given in Figs. 10 and 11, respectively. Again, the theoretical prediction for Λ can be considered as quite satisfactory, but not that for the temperature ratio.

IV. DISCUSSION

A theoretical description of thermal segregation has been explored under very controlled conditions. The fundamental assumptions are the validity of Boltzmann kinetic theory for a binary mixture of inelastic, smooth, hard spheres or disks, and a special exact steady

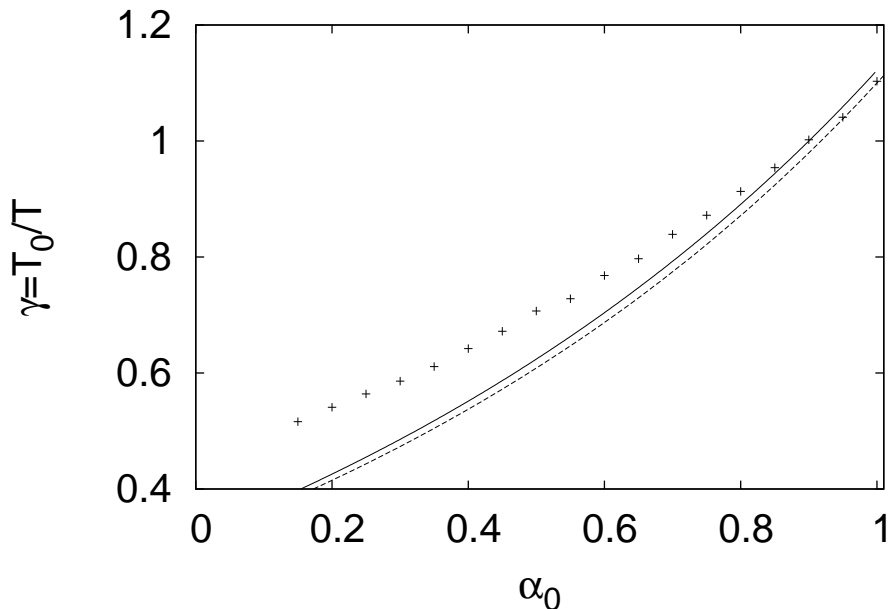


FIG. 6: Ratio between the impurity temperature T_0 and the host gas temperature T in the bulk of the system, once the Fourier state has been reached, as a function of the coefficient of normal restitution for the collisions between the intruder and the host gas particles. The coefficient of normal restitution for the gas is $\alpha = 0.9$. The mass and diameter of the intruder are the same as those of the host particles. The symbols are MD simulation results, the solid line the theoretical prediction from the Boltzmann equation using a truncated Sonine expansion, and the dashed line the weak inelasticity host gas limit given in the Appendix and discussed in the text.

”normal” solution. The kinetic theory is limited to low density gases, which excludes many experimental conditions of interest. However, it provides a useful testing ground for exploring the rather large parameter space of binary mixtures. The normal solution is restricted to conditions for which all space and time dependence can be captured by the hydrodynamic fields, and hence excludes boundary layers as discussed above. The only segregation mechanism considered in the special solution here is a thermal gradient. However, an important feature distinguishing the analysis from others in the literature is the absence of any explicit restriction to small temperature gradients, i.e. a description of thermal segregation outside the Navier-Stokes limit. Still, the absence of solutions for extreme dissipation (see Figs. 1 and 2) suggests an implicit limitation of the normal solution.

As expected, the MD simulation of a finite system with externally imposed temperature

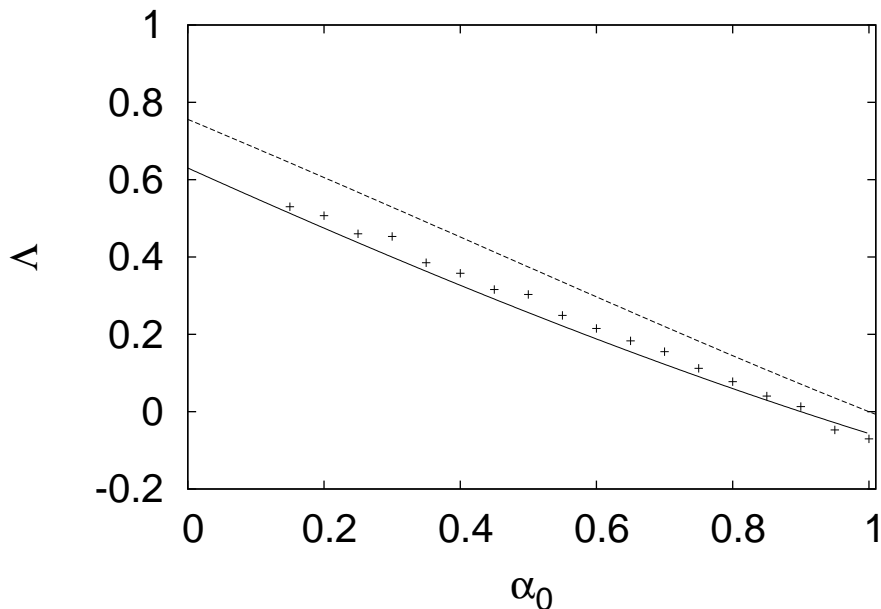


FIG. 7: The dimensionless thermal diffusion factor Δ for the same system as in Fig. 6.

gradient does not give the Fourier state exactly, due to boundary layers. However, in the bulk of the system the Fourier state is confirmed to good accuracy. The comparison of MD and theoretical predictions for the thermal diffusion factor Δ shows good agreement across the parameter space of α_0, m_0, σ_0 . In all cases conditions are found for increased composition of the impurities both along and opposite the temperature gradient. The corresponding comparison for the temperature ratio γ is less satisfactory, particularly for variations of m_0/m and σ_0/σ . It might be taken as a signature of the breakdown of the low order Sonine expansion truncation, but then it is puzzling why this same approximation should work so well for Δ . This discrepancy between theory and simulation for γ remains unexplained at this point.

V. ACKNOWLEDGEMENTS

This research was supported by the Ministerio de Educación y Ciencia (Spain) through Grant No. FIS2011-24460 (partially financed by FEDER funds).

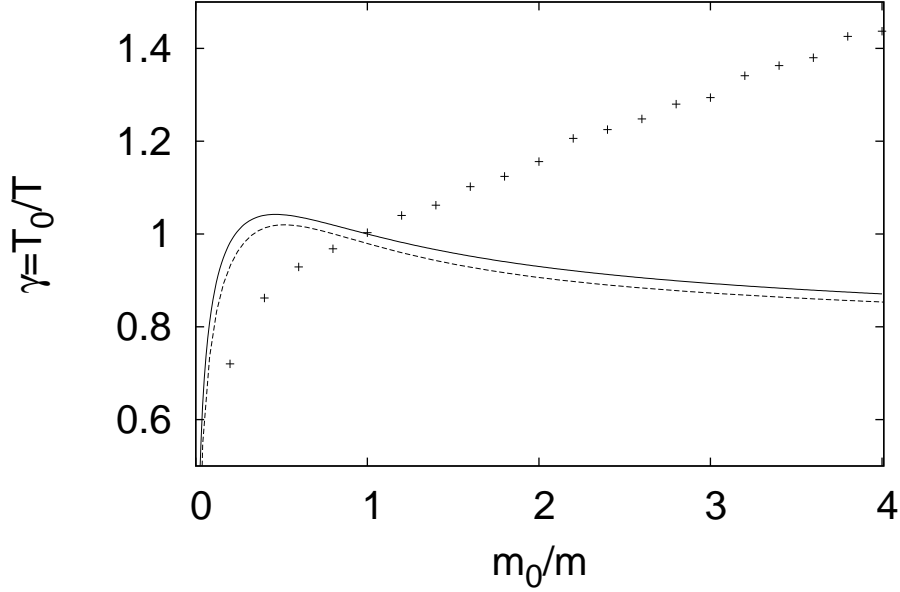


FIG. 8: Ratio between the impurity temperature T_0 and the host gas temperature T in the bulk of the system, once the Fourier state has been reached, as a function of the ratio of the masses m_0/m . The coefficients of normal restitution for the gas-gas and for the gas-intruder collisions are $\alpha = \alpha_0 = 0.9$. The diameter of the intruder is the same as the diameter of the host particles. The symbols are molecular dynamics simulation results, the solid line the theoretical prediction from the Boltzmann equation using a truncated Sonine expansion, and the dashed line the weak inelasticity host gas limit given in the Appendix and discussed in the text.

Appendix A: Nearly elastic host gas limit

The distribution functions of (3) and (6) must be solutions to the Boltzmann and Boltzmann-Lorentz equations, as described in [5]. They are approximated by the truncated Sonine expansions,

$$\begin{aligned} \phi(\mathbf{c}) \simeq \pi^{-d/2} e^{-c^2} & \left[1 - a_{01}(c^2 - dc_x^2) + \left(\frac{d-1}{2} b_{01} + \frac{3}{2} b_{10} \right) c_x \right. \\ & \left. - b_{01} c^2 c_x - (b_{10} - b_{01}) c_x^3 \right], \end{aligned} \quad (\text{A1})$$

$$\begin{aligned} \Phi(\mathbf{c}_0) \simeq \pi^{-d/2} e^{-c_0^2} & \left[1 - A_{01}(c_0^2 - dc_{0x}^2) + \left(\frac{d-1}{2} B_{01} + \frac{3}{2} B_{10} \right) c_{0x} \right. \\ & \left. - B_{01} c_0^2 c_{0x} - (B_{10} - B_{01}) c_{0x}^3 \right], \end{aligned} \quad (\text{A2})$$

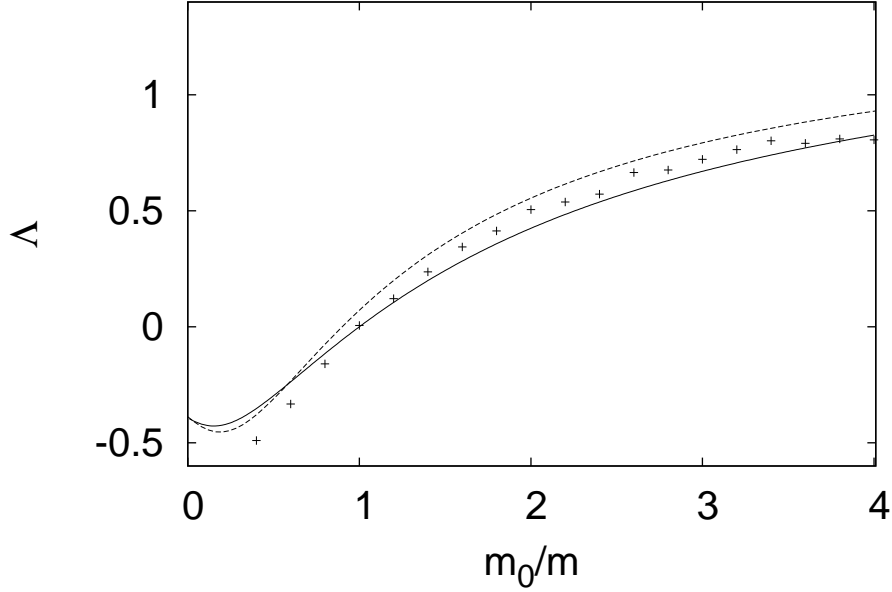


FIG. 9: The dimensionless thermal diffusion factor Λ for the same system as in Fig. 8.

with the constants appearing in these expressions determined from moments of the kinetic equations. For $1 - \alpha \ll 1$ a systematic determination of these coefficients has been carried out for $d = 2$ in the Appendix of [5]. The general results for arbitrary dimension are given here:

$$a_{01} \sim A_{01} = \mathcal{O}(1 - \alpha), \quad (\text{A3})$$

$$b_{01} = b_{10} + \mathcal{O}(1 - \alpha), \quad (\text{A4})$$

$$b_{10} = \left[\frac{2d(1 - \alpha)}{d - 1} \right]^{1/2} + \mathcal{O}(1 - \alpha), \quad (\text{A5})$$

$$B_{10} = B_{01} + \mathcal{O}(1 - \alpha), \quad (\text{A6})$$

$$B_{01} = \frac{16(d - 1)(\sigma/\bar{\sigma})^{d-1} + 27h(2 - h)^{3/2}}{h^{1/2} [24(d + 2) - 8(d + 8)h + 27h^2]} b_{01} + \mathcal{O}(1 - \alpha). \quad (\text{A7})$$

All the dependence on the mass ratio m/m_0 and the coefficient of restitution α_0 occurs through the parameter

$$h \equiv \frac{m(1 + \alpha_0)}{m + m_0}. \quad (\text{A8})$$

Moreover, the coefficients B and C characterizing the hydrodynamic profiles defined in Eqs. (4) and (7) have the expressions

$$B = \frac{2\pi^{\frac{d-1}{2}}(d - 1)}{\sqrt{2}\Gamma\left(\frac{d-1}{2}\right)} b_{01} + \mathcal{O}(1 - \alpha), \quad (\text{A9})$$

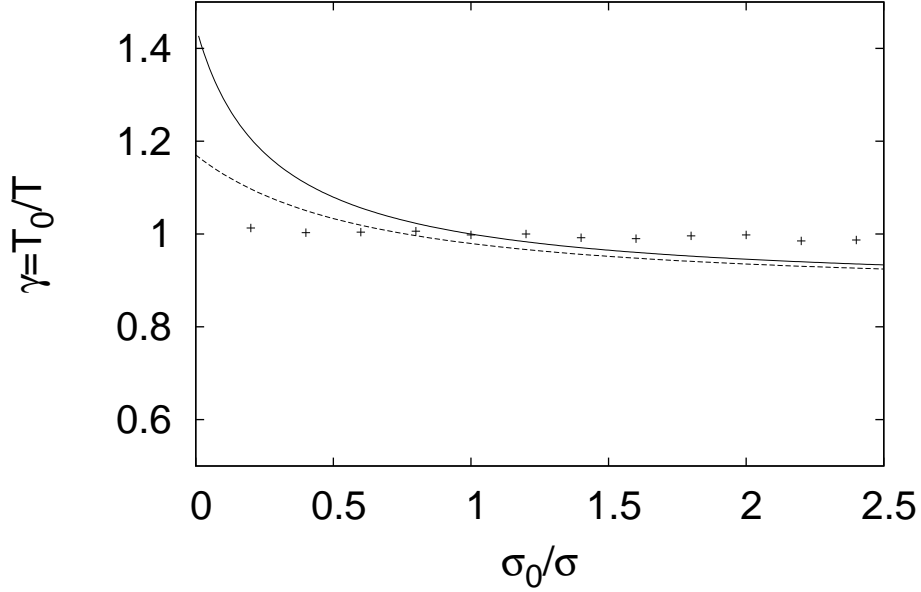


FIG. 10: Ratio between the impurity temperature T_0 and the host gas temperature T in the bulk of the system, once the Fourier state has been reached, as a function of the ratio of the diameters σ_0/σ . The coefficients of normal restitution for the gas-gas and for the gas-intruder collisions are $\alpha = \alpha_0 = 0.9$. The mass of the intruder is the same as the mass the host particles. The symbols are molecular dynamics simulation results, the solid line the theoretical prediction from the Boltzmann equation using a truncated Sonine expansion, and the dashed line the weak inelasticity host gas limit given in the Appendix and discussed in the text.

$$\begin{aligned}
C = & \frac{\pi^{\frac{d-1}{2}}}{16\sqrt{2}\Gamma(\frac{d+4}{2})} \left\{ h^{1/2} [48 + 4d(6 - h) - (56 - 27h)h] B_{01} \right. \\
& - [48(\sigma/\bar{\sigma})^{d-1}(d - 1) \\
& \left. + (2 - h)^{3/2}(8 + 4d + 27h)] b_{01} \right\} + \mathcal{O}(1 - \alpha), \tag{A10}
\end{aligned}$$

while the temperature ratio reads

$$\begin{aligned}
\gamma = & \frac{1 + \alpha_0 - h}{2 - h} \left\{ 1 + \frac{B_{10}}{32d(2 - h)} [(48 + 4d(6 - h) - (56 - 27h)h)B_{01} \right. \\
& \left. - \frac{(2 - h)^{3/2}(8 + 4d + 33h - 6h^2)}{h^{1/2}} b_{01}] \right\} + \mathcal{O}(1 - \alpha)^{3/2}. \tag{A11}
\end{aligned}$$

Notice that all the quantities above have been explicitly evaluated up to order $(1 - \alpha)^{1/2}$, with the exception of the temperature ratio γ that has been computed up to order $1 - \alpha$. Finally, the thermal diffusion coefficient Λ is obtained by substituting Eqs. (A9) and (A10)

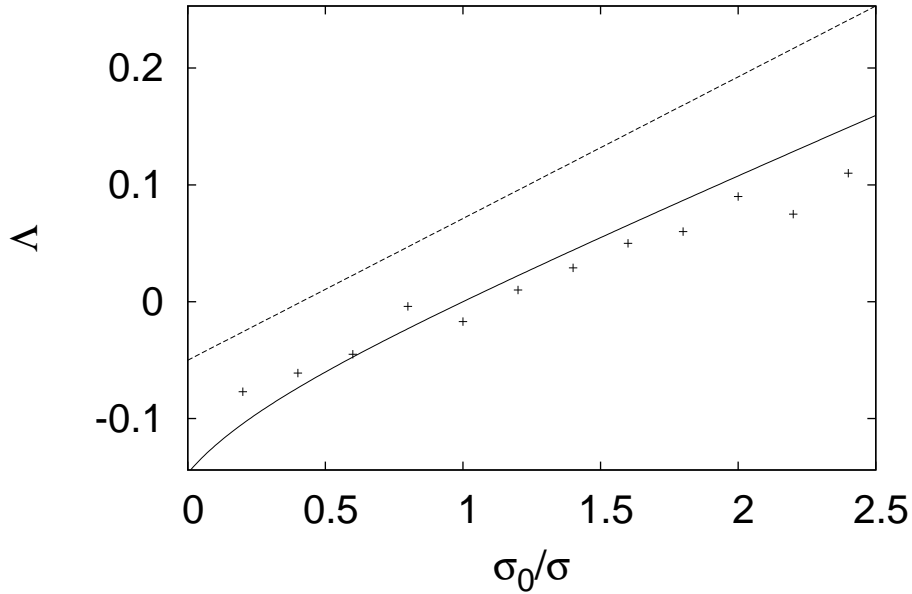


FIG. 11: The dimensionless thermal diffusion factor Δ for the same system as in Fig. 8.

into Eq. (8). This provides an expression valid up to order $(1 - \alpha)^0$.

-
- [1] A. Kudrolli, Rep. Prog. Phys. **67**, 209 (2004).
 - [2] A. Goldshtein and M. Shapiro, J. Fluid Mech. **282**, 75 (1995).
 - [3] J.J. Brey, D. Cubero, F. Moreno, and M.J. Ruiz-Montero, Europhys. Lett. **53**, 432 (2001).
 - [4] J.J. Brey, N. Khalil, and M.J. Ruiz-Montero, J. Stat. Mech. P08019 (2009).
 - [5] J.J. Brey, N. Khalil, and J.W. Dufty, New J. Phys. **13**, 055019 (2011).
 - [6] V. Garzó and F. Vega Reyes, Phys. Rev. E **79**, 041303 (2009).
 - [7] V. Garzó, New J. Phys. **13**, 055020 (2011).
 - [8] J. Duran, J. Rajchenbach, and E. Clément, Phys. Rev. Lett. **70**, 2431 (1993).
 - [9] D.C. Hong, P.V. Quinn, and S. Luding, Phys. Rev. Lett. **86**, 3423 (2001).
 - [10] J.T. Jenkins and D.K. Yoon, Phys. Rev. Lett. **88** 194301 (2002).
 - [11] J.J. Brey, M.J. Ruiz-Montero, and F. Moreno, Phys. Rev. Lett. **95**, 098001 (2005).
 - [12] P. Résibois and M. de Leener, *Classical Kinetic Theory of Fluids* (Wiley-Interscience, New York, 1977).
 - [13] C. Cercignani, *Mathematical Methods in Kinetic Theory* (Plenum, New York, 1969).

- [14] J.R. Dorfman and H. van Beijeren, in *Statistical Physics. Part B*, edited by B.J.Berne (Plenum, New York, 1997).
- [15] E. Livne, B. Meerson, and P.V. Sasorov, Phys. Rev. E **65**, 021302 (2002).
- [16] J.J. Brey, M.J. Ruiz-Montero, F. Moreno, and R. García-Rojo, Phys. Rev. E **65**, 061302 (2002).
- [17] K. Feitosa and N. Menon, Phys. Rev. LEtt. **88**, 198301 (2002).
- [18] V. Garzó and J.W. Dufty, Phys. Rev. E **60**, 5706 (1999).
- [19] J.J. Brey and M.J. Ruiz-Montero, Phys. Rev. E **84**, 031302 (2011).